

Mathematical Models for Sleep-Wake Dynamics: Comparison of the Two-Process Model and a Mutual Inhibition Neuronal Model

A.C. Skeldon*, D.-J. Dijk†, G. Derks*

* Department of Mathematics, University of Surrey, Guildford, Surrey, GU2 7XH,

† Faculty of Health and Medical Sciences, University of Surrey, Guildford, Surrey, GU2 7XH.

July 15, 2014

Abstract

Sleep is essential for the maintenance of the brain and the body, yet many features of sleep are poorly understood and mathematical models are an important tool for probing proposed biological mechanisms. The most well-known mathematical model of sleep regulation, the two-process model, models the sleep-wake cycle by two oscillators: a circadian oscillator and a homeostatic oscillator. An alternative, more recent, model considers the mutual inhibition of sleep promoting neurons and the ascending arousal system regulated by homeostatic and circadian processes.

Here we show there are fundamental similarities between these two models. The implications are illustrated with two important sleep-wake phenomena. Firstly, we show that in the two-process model, transitions between different numbers of daily sleep episodes can be classified as grazing bifurcations. This provides the theoretical underpinning for numerical results showing that the sleep patterns of many mammals can be explained by the mutual inhibition model. Secondly, we show that when sleep deprivation disrupts the sleep-wake cycle, ostensibly different measures of sleepiness in the two models are closely related.

The demonstration of the mathematical similarities of the two models is valuable because not only does it allow some features of the two-process model to be interpreted physiologically but it also means that knowledge gained from study of the two-process model

can be used to inform understanding of the behaviour of the mutual inhibition model. This is important because the mutual inhibition model and its extensions are increasingly being used as a tool to understand a diverse range of sleep-wake phenomena such as the design of optimal shift-patterns, yet the values it uses for parameters associated with the circadian and homeostatic processes are very different from those that have been experimentally measured in the context of the two-process model.

1 Background

Reduced or mis-timed sleep is increasingly recognized as presenting a significant health risk and has been correlated with increases in a diverse range of medical problems including all-cause mortality, cardio-vascular disease, diabetes and impaired vigilance and cognition [1, 2, 3, 4, 5]. The biological mechanisms that result in such problems are beginning to be understood: recent work has shown that changes to the duration or timing of the human sleep-wake cycle can result in the up- or down- regulation and changes to the temporal pattern of large numbers of genes, significantly altering the behaviour of genes associated with biological processes including metabolic, inflammatory, immune and stress responses and circadian rhythmicity [6, 7]. To further understand the underlying phenomena and associations that govern sleep-wake regulation, mathematical models are an important tool to help clarify concepts, challenge accepted ideas and aid in the interpretation of data.

A review of early mathematical models of sleep is given in [8], leading up to the seminal model of Borbély, Daan and Beersma [9, 10], usually called the two-process model, and extended by Borbély and Achermann [11]. As indicated by its name, the two-process model proposes that the sleep-wake cycle can be understood in terms of two processes, a homeostatic process and a circadian process. The homeostatic process takes the form of a relaxation oscillator that results in a monotonically increasing ‘sleep pressure’ during wake that is dissipated during sleep. Switching from wake to sleep and from sleep to wake occurs at upper and lower threshold values of the sleep pressure respectively, where the thresholds are modulated by an approximately sinusoidal circadian oscillator. This model has proved compelling for both its physiological grounding and its graphical simplicity and has been used extensively (there are over 1500 citations to [9] and 600 citations to [10] to-date). For example: to explain why only a relatively short period of recovery sleep is needed to compensate for even lengthy periods of sleep deprivation [9]; to explain chronotype changes in adolescents [12]. Extensions of the two-

process model have been developed to explain the results of chronic sleep restriction experiments [13, 14]. Despite its success, it remains difficult to relate the threshold values in the two-process model and its extensions to physiological processes.

Advances in neurophysiology have led to a proliferation of models that aim to extend the two-process model to a more physiological setting [15, 16, 17, 18, 19, 20, 21]. A recent review is given in [22]. The most extensively tested of these is the model of Phillips and Robinson [17] (the PR model), which has been used to explain sleep fragmentation experiments [23], differences in mammalian sleep patterns [24] and subjective fatigue during sleep deprivation [25]. The PR model has also been extended to allow for the inclusion of the effects of caffeine [26] and to allow for feedback of the sleep-wake cycle on the circadian oscillator in order to explain spontaneous internal desynchrony [27, 28].

In [17, 20], it was observed that the results of their physiologically based models could be presented in a qualitatively similar way as those from the two-process model. Here we show that some features of the PR model are not only qualitatively, but also quantitatively similar to the two-process model: the parameters in the PR model can be explicitly related to the parameters in the two-process model, giving a physiological interpretation to the thresholds in the two-process model. We illustrate the consequences of this explicit relation with two important sleep-wake phenomena. First, by using the fact that the two-process model can be represented as a one-dimensional map with discontinuities [29, 30], we demonstrate how transitions between monophasic and polyphasic sleep occur through grazing bifurcations. These grazing bifurcations are then used to provide a theoretical underpinning for observations that many mammalian sleep patterns can be understood within a common framework by varying just two parameters in the PR model [24]. Second, turning to sleep deprivation experiments, we show how the ‘wake effort’ concept introduced in the PR model to explain sleep deprivation can be explicitly related to the two-process model. This shows that the wake effort is closely related to the difference between the homeostatic pressure and the circadian oscillator, a measure often used in the context of the two-process model to understand sleepiness. Furthermore we discuss briefly how the PR model may explain effects of chronic partial sleep deprivation on waking performance.

2 Sleep models

2.1 The two process model

The two-process model considers a homeostatic pressure $H(t)$ that decreases exponentially during sleep,

$$H(t) = H_0 e^{(t_0-t)/\chi_s} \quad (1)$$

and increases during wake,

$$H = \mu + (H_0 - \mu) e^{(t_0-t)/\chi_w}. \quad (2)$$

The parameter μ is known as the ‘upper asymptote’ [13, 14], this is the value that the homeostatic pressure H would reach if no switch to sleep occurred. Similarly there is a ‘lower asymptote’ of zero. Switching between wake and sleep occurs when the homeostatic pressure $H(t)$ reaches an upper threshold, $H^+(t)$, that consists of a mean value H_0^+ modulated by a circadian process $C(t)$,

$$H^+(t) = H_0^+ + aC(t). \quad (3)$$

The switch between sleep and wake occurs when $H(t)$ reaches a lower threshold, $H^-(t)$,

$$H^-(t) = H_0^- + aC(t), \quad (4)$$

where $C(t)$ is a periodic function of period 24 hours. In the simplest cases

$$C(t) = \sin(\omega(t - \alpha)),$$

but more complicated forms that include higher harmonics, such as

$$\begin{aligned} C(t) = & 0.97 \sin \omega(t - \alpha) + 0.22 \sin 2\omega(t - \alpha) + 0.007 \sin 3\omega(t - \alpha) \\ & + 0.03 \sin 4\omega(t - \alpha) + 0.001 \sin 5\omega(t - \alpha), \end{aligned}$$

have also been used [11]. Typical results of this model illustrating its rich dynamics are shown in Figure 1.

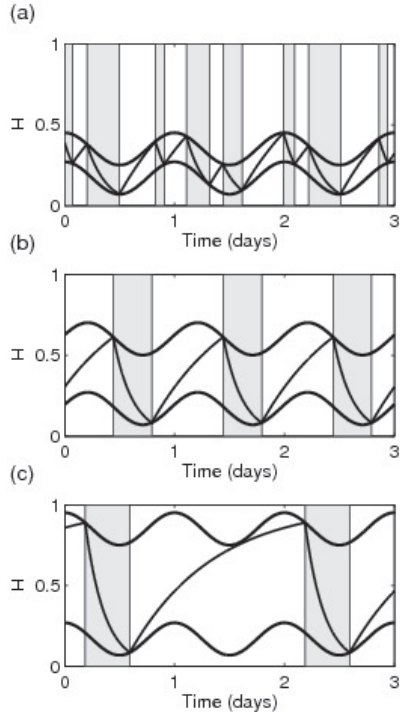


Figure 1: Sleep-wake cycles generated by the two-process model. $C(t) = \sin(\omega t)$, $H_0^- = 0.17$, $a = 0.10$, $\chi_s = 4.2\text{hrs}$, $\chi_w = 18.2\text{hrs}$, $\mu = 1$. (a) $H_0^+ = 0.35$, (b) $H_0^+ = 0.60$, (c) $H_0^+ = 0.85$. Parameters as in [10], Figure 3. The times when sleep occurs (H decreasing) are shaded.

2.2 Phillips and Robinson model (PR model)

At the core of the PR model are two groups of neurons: mono-aminergic (MA) neurons in the ascending arousal system that promote wake and neurons based in the ventro-lateral pre-optic (VLPO) area of the hypothalamus that promote sleep. Phillips and Robinson model the interaction between the MA and the VLPO as mutually inhibitory. In the absence of further effects, this would mean that the model would either stay in a state with the MA active (wake) or in a state with the VLPO active (sleep) and no switching between the states would occur. Switching between sleep and wake occurs because the model also includes a drive to the VLPO that is time dependent and consists of two components: a circadian drive, $C(t)$, and a homeostatic drive $H(t)$. The structure of the PR model is shown in Figure 2(a).

The neurons are modelled at a population level and are represented by

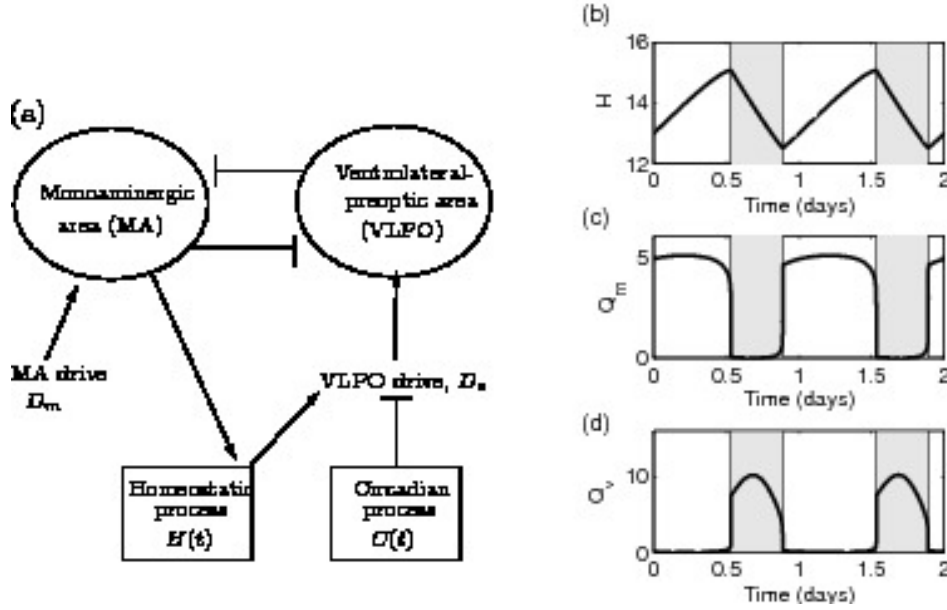


Figure 2: (a) Diagrammatic description of the PR model showing the links between the VLPO, MA, the homeostatic and the circadian processes. (b), (c) and (d) show typical timeseries for the level of the homeostat, H , and the firing rates of the MA and VLPO, Q_m and Q_v , respectively. The times where sleep occurs are shaded.

their mean cell body potential relative to rest, V_j for $j = m, v$, where v represents the VLPO group and m represents the MA. The potential is related to the firing rates of the neurons by the firing function, Q_j ,

$$Q_j = \frac{Q_{\max}}{1 + \exp[-(V - \theta)/\sigma']}, \quad (5)$$

where Q_{\max} is the maximum firing rate and θ is the mean firing threshold relative to resting. The function Q_j is a sigmoid function, which is close to zero for all negative values of V_j and then saturates exponentially fast to Q_{\max} .

The neuronal dynamics are represented by

$$\begin{aligned} \tau_v \dot{V}_v + V_v &= -\nu_{vm} Q_m + D_v, \\ \tau_m \dot{V}_m + V_m &= -\nu_{mv} Q_v + D_m, \end{aligned} \quad (6)$$

where the drive to the VLPO, D_v and to the MA, D_m are given by

$$\begin{aligned} D_v &= \nu_{vh} H - \nu_{vc} C - A_v, \\ D_m &= A_m. \end{aligned}$$

The homeostatic component of the drive, H is modelled by

$$\chi\dot{H} + H = \bar{\mu}Q_m, \quad (7)$$

and the circadian drive, C , is approximated by

$$C(t) = \cos(\omega(t - \alpha)),$$

where $\omega = 2\pi/24 \text{ hrs}^{-1}$ and α is a shift that specifies the distance from the circadian maximum. Typically, α is chosen so that the switch from sleep to wake occurs at an appropriate clock time.

Typical results produced by the PR model are shown in Figure 2(b)-(d). During wake, the firing rate of the MA neurons is high ($Q_m \approx 5 \text{ s}^{-1}$), that of the VLPO is low and the homeostatic pressure tends to increase, while during sleep the firing rate of the MA neurons is low ($Q_m \approx 0 \text{ s}^{-1}$), that of the VLPO is high and the homeostatic pressure tends to decrease. Note that in the PR model switching between wake and sleep is defined to occur when Q_m reaches the threshold value of one; this differs from the timing of the maximum and minimum homeostatic pressure by a few minutes. Obviously, the exact choice of the threshold does not play an important role in the dynamics of the system, but does change the regions that are labelled as sleep or wake.

3 Comparison of the PR and two-process models

As recognised in [23], since changes in neuronal potentials happen much faster than changes associated with the homeostatic pressure, $\tau_j \ll \chi$, there is a strong separation of timescales in the PR model. This strong separation of timescales means that the dynamics of the PR model is well approximated by two separate models: one on the ‘slow’ timescale that is appropriate when considering changes on the timescale of the circadian and homeostatic processes such as the timings of sleep and wake; and the other, the ‘fast’ timescale, which is appropriate when considering changes on the timescale of the neuronal potentials such as the response to a night time disturbance. If the firing switching function Q_j given in equation (5) in the PR model is replaced by a hard switch,

$$Q_j = \begin{cases} 0 & \text{for } V_j < \theta_S \\ Q_S & \text{for } V_j \geq \theta_S, \end{cases} \quad (8)$$

where Q_S is the mean maximum firing rate of the neuronal population and θ_S is the value at which the switch occurs, we show in Appendix B that the parameters for the slow dynamics of the PR model with a switch can be exactly mapped to parameter values in the two-process model, specifically,

$$\begin{aligned} H_0^+ &= \frac{\theta_S + A_v + \nu_{vm}Q_S}{\nu_{vh}}, & H_0^- &= \frac{\theta_S + A_v}{\nu_{vh}}, \\ a &= \frac{\nu_{vc}}{\nu_{vh}}, & \mu &= \bar{\mu}Q_S, & \chi_s = \chi_w &= \chi. \end{aligned} \quad (9)$$

The lower threshold is therefore dependent on the mean drive to the VLPO and the threshold firing rate. The difference between the thresholds in the two-process model,

$$H_0^+ - H_0^- = \frac{\nu_{vm}Q_S}{\nu_{vh}},$$

can then be interpreted physiologically as the amount by which the MA inhibits the firing of the VLPO during wake. This makes intuitive sense: there is hysteresis in the switch between wake and sleep because of the mutual inhibition between the MA and the VLPO. In the wake state, the VLPO requires a large drive to fire to counteract the inhibitory effects of the MA. Once in the sleep state, less drive is needed to maintain firing because the MA is quiescent.

Using the standard parameters for the PR model, only a small part of the firing function (5) is used. This is illustrated in Figure 3(a), where the

firing function is shown by the dashed line and the typical range of values for Q_m is shown by the thick line. We show in Appendix C that there is a systematic way to relate the parameters for the original PR model to equivalent parameters for the two-process model that retain the timings and values at the extrema of the homeostat. In keeping with the fact that the mean firing rate across the neuronal population Q_S is much less than the maximum possible firing rate Q_{\max} , the value for Q_S is significantly less than Q_{\max} but close to the mean firing rate across the population in the PR model: in fact the actual firing function needed in the PR-switch model is shown by the thin line in Figure 3(b).

Typical graphs of H and Q_j for both the original PR model and the PR switch model are shown in Figure 3(c)-(e) demonstrating the close agreement between the two cases. Graphs comparing timeseries computed from the two-process model and numerical integrations of the corresponding PR/PR switch model are shown in Figure 4. The extremely good agreement of the two models is a result of the very large disparity in timescales between the fast and slow systems. Consequently, solutions of the PR model converge to solutions on the slow manifold on the timescale of minutes. Once on the slow manifold, solving the PR model is essentially equivalent to solving the two-process model.

In [31] it was recognised that the PR model could be plotted in a similar way to the two-process model, but the explicit connection between parameters was not made. It is stated that a key difference is that in the two-process model the value of H remains between the thresholds at all times, as in Figure 1. However, we note that this could be regarded as a matter of parameter choice rather than a fundamental difference between the two models: whether the two-process model remains between the thresholds depends on the relative gradients of the circadian and homeostatic processes at each wake/sleep or sleep/wake transition. Figure 4 shows that, with the PR parameters used to model sleep regulation in humans, the two thresholds in the two-process model are very close, hence the circadian oscillation is the dominant sleep regulator and the two thresholds merge almost into one.

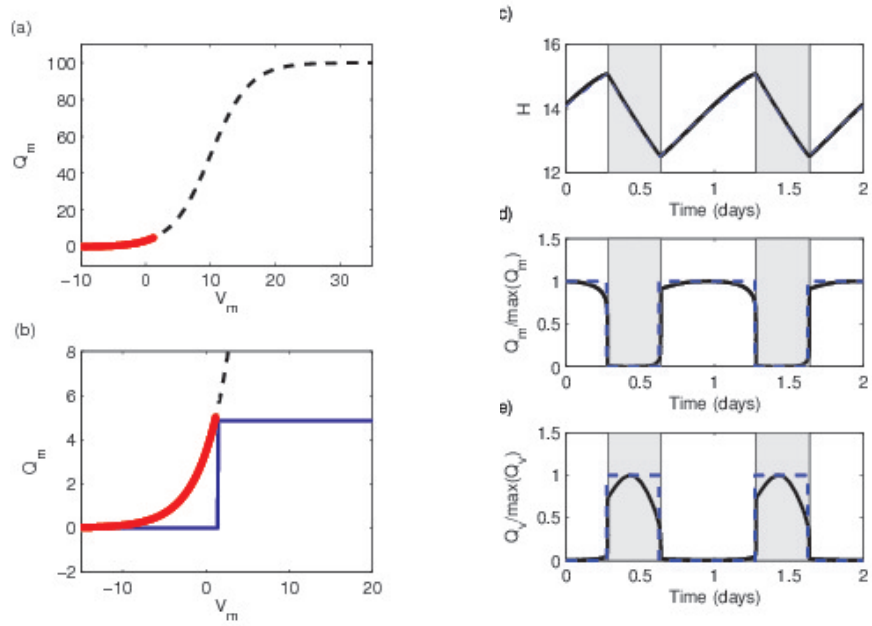


Figure 3: (a) The dashed (black) line shows the firing function given by equation (5); the thicker (red) line shows the portion that is used for the ‘normal’ PR cycle. (b) A magnified version of (a). The thin (blue) line shows the switch function (8). Panels (c),(d) and (e) show the behaviour of the homeostat, H , and the firing rates Q_m and Q_v for the PR model (solid line) and the PR model with the hard switch (dashed line). The switch parameters are $\theta_S = 1.45\text{mV}$, $Q_S = 4.85\text{s}^{-1}$, the mean firing rate of the neural population during wake; all other parameters are listed in Appendix A.

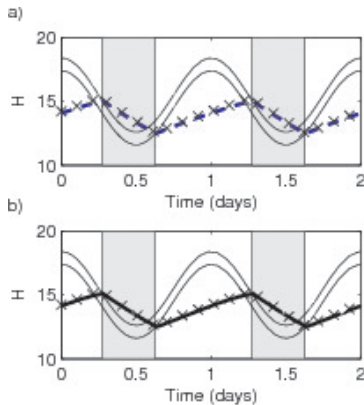


Figure 4: (a) Comparison of the PR switch model with the two-process model. (b) Comparison of the PR model with the two-process model. Crosses show the two-process model; solid line the PR model and (blue) dashed line the PR switch model.

4 The two-process model re-visited

The link between the PR model and the two-process model not only gives us a physiological interpretation of the thresholds in the two-process model, it also allows us to gain a greater insight into the dynamics of the PR model, enabling understanding developed in the context of the two-process model to be interpreted in the physiological setting of the PR model. In this section, two different examples are discussed.

4.1 Transitions from monophasic to polyphasic sleep

It is well-known that the two-process model can show a range of different sleep-wake cycles, including cycles that have multiple sleep episodes each day, see Figure 1(a), and cycles that have a period greater than one day, see Figure 1(c). Indeed in [10], the authors postulate that the two-process model can explain the polyphasic sleep of many animals. In [24], it is shown that the sleep-wake cycles of many different mammals can be understood by varying two parameters in the PR model: the homeostatic time constant χ and the constant component to the VLPO drive, A_v . In the previous sections, we have demonstrated how the parameters of the PR model relate to those of the two-process model, specifically, the homeostatic time constant χ is present in both models and varying the drive to the VLPO A_v corresponds to varying the upper and lower thresholds without changing the distance between them. In [29, 30] it is shown that the two-process model can be

understood as a one-dimensional map with discontinuities. In this section, we use this map to show how the observations in [24] and the postulate in [10] are linked and clarify how the transition between different numbers of daily sleep episodes occurs.

First we introduce the one-dimensional map. Consider the two-process model and suppose we start on the upper threshold, at time T_0^0 , where the model switches from wake to sleep. The dynamics of the two-process model takes this starting point and, propagating it forward through one sleep and one wake episode, results in the next wake to sleep time, T_0^1 , and then through a further sleep-wake episode to T_0^2 and so on, generating a sequence of sleep onset times $T_0^1, T_0^2, T_0^3 \dots$. This is illustrated for $T_0^0 = 0$ days in Figure 5(a). Different starting values T_0^0 generate different sequences of sleep times, as illustrated in Figure 5(b). For the parameter values chosen here, all sequences converge rapidly to the same monophasic periodic cycle. A graphical way of understanding this sequence is to plot T_0^{n+1} modulo 1 day against T_0^n modulo 1 day (the first return map). For any particular starting value, the sequence of iterates can then be found by drawing the cobweb diagram, as shown in Figure 5(d). A monophasic sleep pattern corresponds to $T_0^{n+1} = T_0^n$ modulo 1 day and so corresponds to the intersection of the diagonal line with the map. The fact that the sequences converge rapidly is related to the fact that the gradient of the map is close to zero for most values of T_0^n . This rapid convergence means that a temporary change to timing of sleep will revert to the regular sleep-wake cycle within a few days.

Phrasing the two-process model in these terms illustrates that it can be represented as a one-dimensional map. Probably the most well-known example of such maps is the logistic map [32] which has been widely used to show that simple rules can lead to very complex dynamics. A distinctive feature of the two-process model is the fact that the map contains a discontinuity. For the parameter values shown in Figure 5(d) this discontinuity occurs at $T_0^0 \approx 0.95$ days. The discontinuity is a consequence of the fact that there exist neighbouring starting values T_0^0 that lead to trajectories that follow very different paths. These occur whenever there are points that result in trajectories that become tangent to the thresholds. For example, starting at $T_0^0 = 0.96$ days, the first sleep just misses the wake threshold at 1.08 days so remains asleep until 1.6 days resulting in a sequence $0.96, 1.6, \dots$, as shown in Figures 5(b) and (c); whereas starting at the nearby value of $T_0^0 = 0.92$ days, the trajectory hits, rather than misses, the sleep threshold and the resulting sequence is $0.92, 1.1, \dots$

For the value of the clearance parameter $\chi = 45$ hrs used in Figure 5, the discontinuity does not have a significant impact on the dynamics and all trajectories converge rapidly to the same periodic cycle. However, the

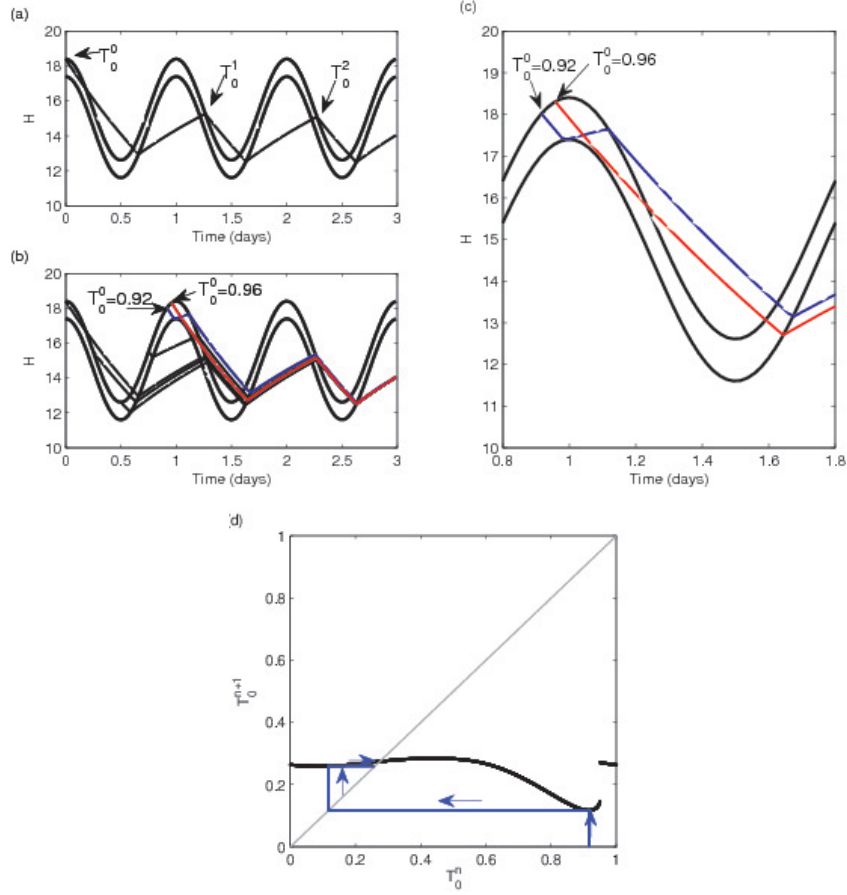


Figure 5: (a) A single trajectory of the two-process model showing successive times of sleep onset. (b) Trajectories of the two-process model for different initial sleep onset times. Each different sleep onset time results in a different sequence, $T_0^0, T_0^1 \dots$, but each sequence rapidly converges to the same sleep onset time, of 0.27 modulo 1 day. (c) A zoom of (b), showing only the trajectories for $T_0^0 = 0.92$ days and $T_0^0 = 0.96$ days. (d) First return map for the two-process model. The black line shows the return map, in other words for any value of sleep onset time on day n , T_0^n it shows the onset time of sleep on day $n + 1$, T_0^{n+1} . The grey diagonal line is the line along which $T_0^n = T_0^{n+1}$. One typical trajectory is plotted for $T_0^0 = 0.92$ showing the rapid convergence to the periodic cycle where $T_0^n = T_0^{n+1} = 0.27$ modulo 1 day, the point at which the return map and the diagonal line intersect. The discontinuity is a result of the fact that neighbouring values of T_0^n exist that lead to very different values for T_0^{n+1} , as shown in (c). Parameter values for the two-process model are based on the PR model for the human sleep-wake cycle and can be found in Appendix C.

presence of the discontinuity is key to understanding the transition from monophasic to polyphasic sleep. This is illustrated in Figure 6(a)-(d), where a sequence of converged solutions to the two-process model are shown for decreasing χ . For $\chi = 20$ hrs, the sleep-wake cycle is monophasic, but in the wake episode the trajectory comes close to, but just does not touch, the upper threshold (Figure 6(a)). If distance from the upper threshold is a measure of sleepiness during wake, this would correspond to a dip in alertness. If χ is reduced further, say to $\chi = 18$ hrs as shown in Figure 6(b), then the wake trajectory does not only come close to, it touches the upper threshold resulting in a short nap and a sleep-wake cycle that is bi-phasic with one longer sleep and one short sleep. Decreasing χ further results in a sequence of further tangencies each of which adds one additional sleep-wake episode. Such transitions are known as grazing bifurcations, tangent bifurcations, or border collision bifurcations and are characteristic of one-dimensional maps with discontinuities [33, 34, 35]. In the return map, a grazing bifurcation occurs when the discontinuity in the map coincides with the diagonal line. They are responsible for period-adding transitions in the context of electronic circuits and here, we see, are responsible for sleep-episode-adding transitions. Such transitions have also been observed and analysed using one-dimensional maps in the context of understanding the dynamics of neurons [36, 37].

The sleep-wake pattern for varying χ is shown in Figure 6(e). For larger values of χ there is one episode of sleep each day: the model falls asleep exactly once and always at roughly the same time ($N = 1$). A grazing bifurcation occurs at around $\chi = 19.8$ hrs and results in a region between $15 < \chi < 19$ hrs where sleep is bi-phasic with one longer and one shorter sleep each day ($N = 2$). A succession of further grazing bifurcations take place as χ is reduced, resulting in increasing numbers of daily sleep episodes. From Figure 6(e) we see there are intermediate regions between each value of N . For example, between the monophasic and biphasic region there is a small region around $\chi = 19.8$ hrs where the sleep pattern has a period of two days. This corresponds to a region where a grazing bifurcation has taken place, causing an extra sleep period on one day, but this extra sleep period is enough to mean that no additional sleep is needed on the following day. The sleep wake trajectory in this case is shown in Figure 7(a). Similar behaviour is seen at each transition between different numbers of daily sleep episodes and is characteristic of such transitions in one-dimensional discontinuous maps [38]: this is illustrated for the transition between two and three sleep episodes in Figures 7(b) and a similar pattern of sleep to that shown in Figure 1(a) using parameters as in [10]. In fact, as shown for one-dimensional discontinuous maps in [38], the situation is even more complicated: in Figure 1 of [27] the first few layers of an infinite adding scheme are set out. This

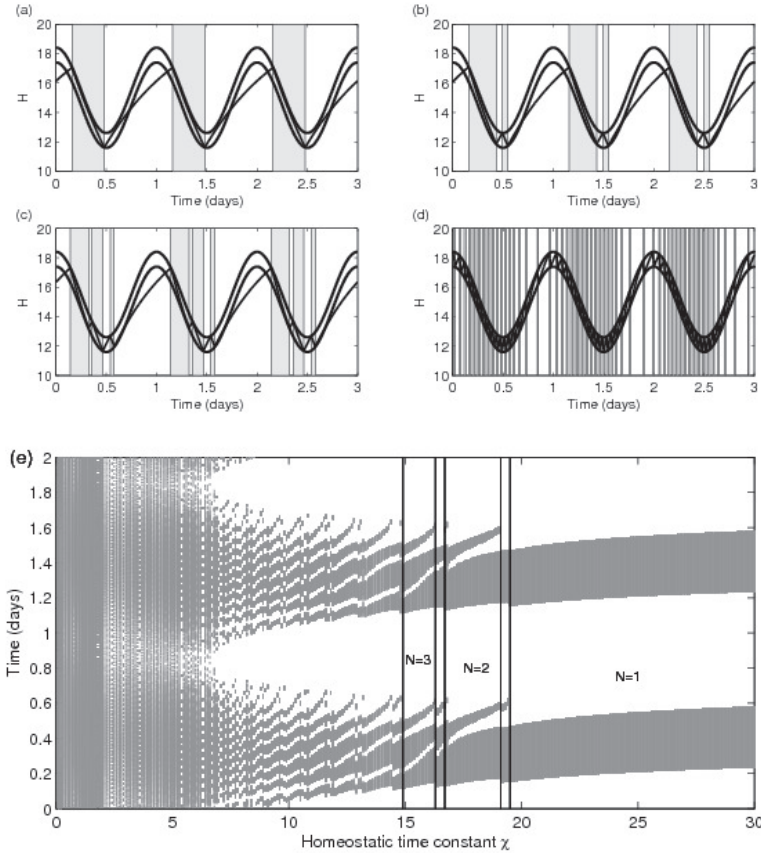


Figure 6: Using the two-process model with parameters as indicated in Appendix C, Figures (a)-(d) give sleep-wake cycles for different values of the homeostatic time constant χ ($\chi = 20, 18, 16, 5$ hrs), illustrating that reducing χ results in more daily sleep episodes. (e) Sleep regions (shaded) as a function of χ . Note that the circadian maximum occurs at $t = 0, 1, \dots$ days.

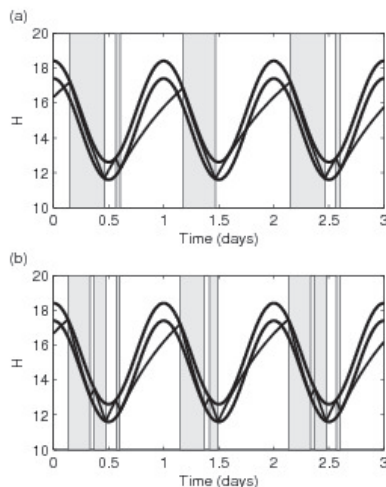


Figure 7: Solutions of the two-process model showing periodicity on the period of two days. (a) $\chi = 19.3$ hrs (b) $\chi = 16.6$ hrs. All other parameters are as in Figure 6 and can be found in Appendix C.

shows that, for example, the sequence of transitions from sleeping once a day to sleeping twice a day is $\{1, 1, 1, \dots\} \dots \{1, 1, 2, 1, 1, 2 \dots\}$, $\{1, 2, 1, 2 \dots\}$, $\{1, 2, 2, 1, 2, 2, 1 \dots\} \dots \{2, 2, 2, \dots\}$, etc.

Further discussion of the map is given in the Supplementary Material.

In [24], the behaviour of the PR model is examined both as the time constant χ and the mean drive to the VLPO, A_v are varied. Our parameter equivalences between the PR model and the two-process model (9) show that increasing A_v is equivalent to increasing the upper and lower thresholds without changing the distance between them. One can then deduce for the two-process model that for low A_v , the homeostat will never reach the lower threshold and no wake will occur. Similarly, for high A_v no sleep will occur. For large values of χ (χ greater than approximately 20 hrs), the amount of daily sleep varies approximately linearly with the mean drive to the VLPO as shown in Figure 8(a) and observed in [24]. As seen before, the sleep-wake cycle is monophasic and is largely independent of χ in this range. The actual transition between monophasic sleep and no sleep (or no wake) occurs through grazing bifurcations, where this time the grazing bifurcations result in periodic cycles that have wake (sleep) episodes of greater than 24 hours: examples of such cycles are evident in Figure 8(a) at the extremes of the values of A_v that are shown. For smaller values of χ , where polyphasic sleep exists, varying A_v shows that, as the no sleep (or no wake) threshold are

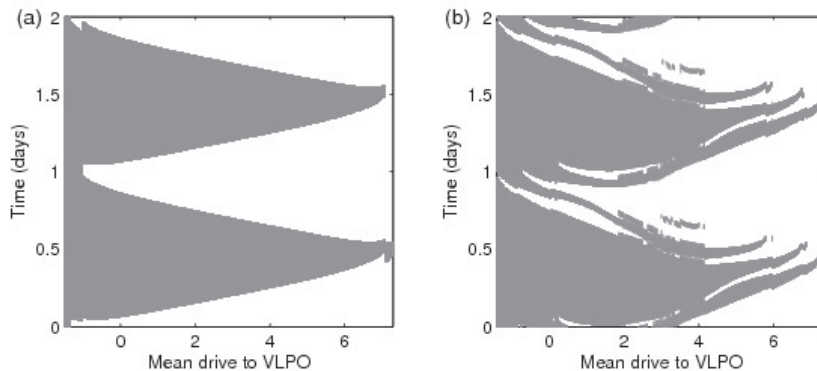


Figure 8: Sleep timing in the two-process model while simultaneously varying the upper and lower thresholds via $H_0^- = 1.45 + A_v$ and $H_0^- = 2.46 + A_v$ with (a) $\chi = 45$ hrs (b) $\chi = 15$ hrs and all other parameters as in Appendix C. Note that mean VLPO drive equals $c_0 = A_v/\nu_{vc}$ for consistency with [24]. Sleep regions are shaded.

approached, grazing bifurcations result in ever decreasing numbers of sleep (wake) episodes until no sleep (no wake) occurs, see Figure 8(b).

In [24], it was shown that the sleep of many mammalian species could be understood in the context of the PR model by varying just two, physiologically plausible, parameters: χ and $c_0 = A_v/\nu_{vc}$. Their results show: a sequence of transitions from monophasic to polyphasic sleep as the time constant χ is reduced but where total sleep daily sleep remains approximately constant; for fixed χ and varying mean drive to the VLPO a sequence of transitions from a state with no wake to a state with no sleep. By using the relationship between the PR model and the two-process model we see that reducing χ results in a sequence of transitions from monophasic to polyphasic sleep through grazing bifurcations that successively add sleep episodes; at the transition between N episodes of sleep and $N + 1$ episodes of sleep, there are regions where sleep alternates between N and $N + 1$ daily episodes (examples of such trajectories for the PR model are shown in the Supplementary Material). The parameter equivalences identified in Section 3 show that changing the mean drive to the VLPO is equivalent to simultaneously shifting the upper and lower thresholds of the two-process model. The relation between the PR model and the two-process model shows how this inevitably leads to grazing bifurcations and ultimately cycles with either no sleep or no wake.

The quantitative agreement is close with [24], but not exact: this is because we have chosen a fixed value for μ , the upper asymptote, in the two-

process model, the value to match the PR model for $\chi = 45$ hrs. Varying χ in the PR model results in a small change to the precise region of the switching function that is used, which in turn induces some change in the value of Q_S . Since $\mu = \bar{\mu}Q_S$ this results in some dependence of μ on χ in the equivalent two-process model. One consequence is that the switch from monophasic sleep to biphasic sleep occurs at around $\chi = 19$ hrs for the two-process model instead of $\chi = 16$ hrs for the PR model. More details can be found in the Supplementary Material.

4.2 Wake effort

Sleep deprivation experiments involve keeping subjects awake for an extended period of time during which cognitive and behavioural tests are undertaken to measure sleepiness and performance. One measure of sleepiness is the Karolinska Sleepiness Scale (KSS) score and in [25], the concept of ‘wake effort’ is introduced for the PR model and good agreement between wake effort and experimental data on KSS scores is found. Wake effort corresponds to a change in the drive to the MA and is interpreted as a need to provide the MA with greater stimulation in order to maintain wake. Here, we show how this can be re-interpreted in the context of the two-process model.

Wake effort in [25] is presented by considering the graph of the MA firing rate Q_m (or equivalently, V_m), against the drive to the VLPO, D_v . In a regular sleep-wake cycle, Q_m follows a hysteretic loop, see Figure 9(a), where the transition from wake to sleep occurs close to D_v^+ and the transition from sleep to wake occurs close to D_v^- . During sleep deprivation, it is argued in [25] that by increasing D_m , rather than switch from wake to sleep, it is possible to stabilise the ‘ghost’ of the wake state: the extent to which D_m is increased is known as the wake effort. An alternative view of the same idea is to consider the (D_m, D_v) -plane as shown in Figure 9(b) and recognise that D_v^\pm are curves that divide the parameter plane into regions where only the wake state exists, only the sleep state exists, and a bistable region where both wake and sleep exist. There are also regions for low D_m ($D_m < 0.4$ mV) and high D_m ($D_m > 200$ mV) where the two states cannot readily be distinguished. The region of relevance for the parameters used in [25] is close to the bottom of the bistable region, and is shown in blow-up in Figure 9(c). The horizontal line represents the normal sleep-wake cycle: the time dependence of the homeostatic and circadian processes result in D_v oscillating backwards and forwards along the line, switching from wake to sleep for increasing D_v when $D_v = D_v^+$ and from sleep to wake for decreasing D_v when $D_v = D_v^-$.

In sleep deprivation experiments, subjects are prevented from falling asleep at $D_v = D_v^+$. At this point, in order to remain awake the only al-

alternatives that keep the system in the wake region are: decrease the drive to the VLPO, D_v ; increase the drive to the MA, D_m or some combination of both of these. In [25], it is argued that in order to maintain wake it is necessary to stimulate the MA, and therefore D_m is increased to remain on the ‘ghost state’, but this is equivalent to following the line D_v^+ . The additional amount by which the MA is stimulated, the wake effort, W is then

$$W = D_m^+ - 1.3,$$

where D_m^+ is a function of D_v^+ and is the solution of equations (14) in Appendix C. For the region of relevance shown in Figure 9(c) and (d), the relationship is close to linear with a small quadratic term and is well-approximated by

$$D_m^+ \approx -0.012D_v^{+2} + 0.416D_v^+ + 0.383.$$

In the two-process model, acute sleep deprivation is modelled as a continued increase in the homeostatic pressure. In [10] this is interpreted as a suspension of the upper threshold, but with insight gained from the PR model, we see that an alternative interpretation is that the upper threshold is continuously moved to keep the model in the wake state, as shown in Figure 10(a). The wake effort is then related to the extent to which the threshold has to be moved, that is the quantity $\max(H - H^+, 0)$ with the upper threshold H^+ as given by (3). This quantity is shown in Figure 10(b). Using the explicit relationships between the parameters in the PR model and the two-process model, the moving of the threshold corresponds to a modified value for D_v^+ is given by $D_v^+ = H - H^+ + 2.46$, as $\nu_{vh} = 1$ and $2.46 = \nu_{vh}H_0^+ - A_v$, the value of D_v^+ if no wake effort is applied, so the wake effort for the two-process model is

$$W \approx -0.012 (H - H^+)^2 + 0.357 (H - H^+). \quad (10)$$

This resulting wake effort computed from the two-process model is shown by the solid line in Figure 10(c) and agrees very well with the calculation of the wake effort from the PR model in [25] (crosses).

The close to linear relationship (the quadratic term has a very small coefficient) between wake effort in the PR model and $H - H^+$, which is essentially the difference between the homeostatic pressure and the circadian oscillator, demonstrates that the wake effort used in [25] is fundamentally similar to previous measures used to compare performance and sleepiness scores. The precise scaling relationship and the degree of nonlinearity is dependent on the shape of the bistable region in the (D_m, D_v) -plane shown

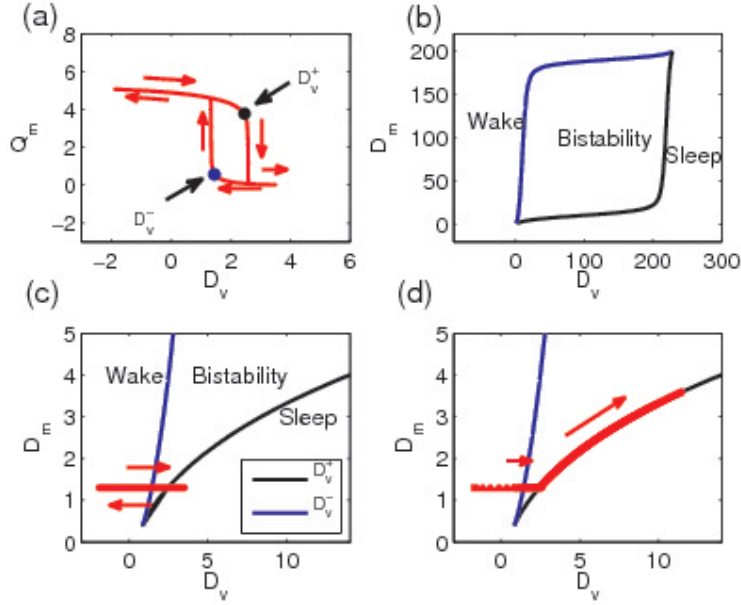


Figure 9: (a) Sleep-wake cycle showing the MA firing rate Q_m as a function of the drive to the VLPO D_v . Over one cycle D_v oscillates between high and low values. When D_v is low, Q_m is high and the model is in a wake state. When D_v is high, Q_m is low and the model is in a sleep state. The transitions from wake to sleep and sleep to wake occur at D_v^+ and D_v^- respectively. The size of the hysteresis loop depends on D_m , shrinking to nothing for $D_m < 0.4$ mV and for $D_m > 200$ mV. (b) The path of D_m^+ and D_m^- in the D_m, D_v plane. D_m^+ and D_m^- do not exist for values of D_m that are either less than 0.4 mV or greater than 200 mV. Consequently for $D_m < 0.4$ mV or $D_M > 200$ mV increasing D_v will result in a smooth change from high Q_m (wake) to low Q_m (sleep) instead of the jump from one state to the other shown in (a). (c) A blow up of (b), with the ‘normal’ sleep-wake cycle superimposed. (d) The D_m, D_v plane showing the wake trajectory in a sleep deprivation experiment.

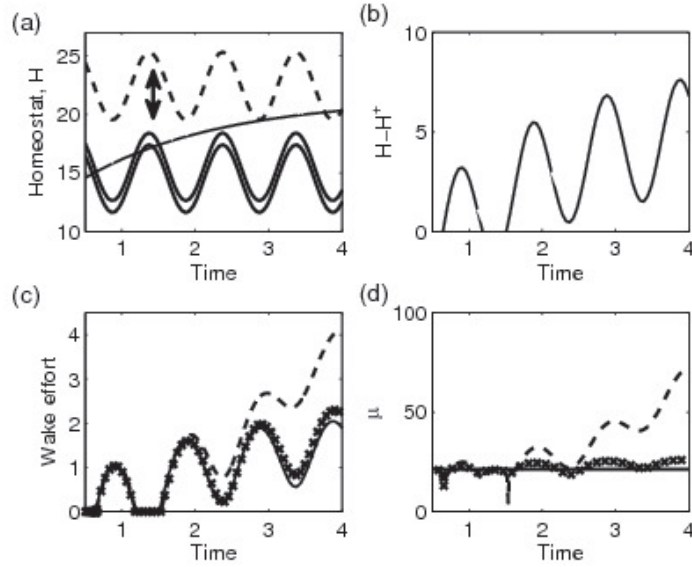


Figure 10: (a) The two-process model, showing the typical trajectory of the homeostatic pressure during a sleep deprivation experiment. Using the wake effort concept of [25] suggests that the upper threshold moves simultaneously: the dashed line shows the position of the upper threshold after 4 days. (b) The difference between the homeostatic pressure and the value at the ‘normal’ threshold, $H - H^+ = H(t) - (H_0^+ + aC(t))$. (c) The wake effort computed from the two-process model (10) (solid line), the PR model as in [25] using $\mu = \frac{\bar{\mu}Q_m^2}{\nu_h + Q_m^2}$ (crosses), the PR model with $\mu = \bar{\mu}Q_m$ (dashed line). (d) The dependence of μ , the upper asymptote, on time for the three different cases shown in (c). The downward spikes indicate that the model gets very close to falling asleep, hence Q_m gets very close to 0.

in Figure 9(b), and on the choice of function for the dependence of the homeostatic process on the firing rate of the MA. In [17] and for many of the subsequent papers, the upper asymptote is given by $\mu = \bar{\mu}Q_m$. However, in [25] the functional form $\mu = \bar{\mu} \frac{Q_m^2}{\nu_h + Q_m^2}$ is used in order to "limit the unrealistically high production rate at high Q_m ". This change in functional form has the effect of keeping μ approximately constant during wake, which is why the agreement between the wake effort as defined by [25] agrees well with our analogous computation from the two-process model. This is illustrated in Figure 10(c) and (d) where the wake effort and the dependence of μ on time are shown for the two-process model and for the PR model with the two different functional forms for μ .

The shape of the bistable region in the (D_m, D_v) plane shows that for D_m larger than about 30 mV, there is a transition from relatively small changes in D_m needed to maintain wake to very large changes in D_m needed to maintain wake; eventually it becomes impossible to maintain wake at all. While for typical parameters used in the PR model this transition occurs for infeasibly large values of D_v and D_m , we note that the shape of the bistable region is dependent on the parameters within the firing function and the choice of firing function itself. Once fixed in [31] these parameters have largely been left unchanged: we will return to this point in the discussion.

5 Discussion

The strengths of the two-process model have been its inclusion of the two fundamental processes that are believed to regulate the sleep-wake cycle along with its graphical simplicity. This has meant that it has been used extensively as a tool to understand the behaviour of the sleep-wake cycle, design experiments and interpret data [39, 40]. A weakness is the difficulty in relating the threshold levels of the homeostatic pressure H that result in switches between wake and sleep to physiological quantities.

The PR model was developed with the same two governing processes in mind, but introduced some physiological basis for the switching that occurs between wake and sleep. In recent years, this model has been extensively tested in a range of scenarios, some of which depend on the fast dynamics within the model, like the role of disturbances during sleep [23], but in many cases relying on the slow dynamics of the model. The four orders of magnitude between the neuronal timescale and the homeostatic/circadian timescales means that the timescale separation between the slow and fast dynamics is very good.

Here we have shown that the slow dynamics of the PR model can be explicitly related to the two-process model, which provides new perspectives on

both the two-process model and the PR model. Using this relationship, new insight into the meaning of the two-process model has been gained. Specifically, the distance between the thresholds is related to the degree to which the MA inhibits the VLPO during wake and the values of the thresholds are related to the parameters associated with the modelling of the firing rates Q_j , the mean VLPO drive, and the strength of the homeostat. The parameter comparison also highlights the fact that there is no strong reason why the homeostatic pressure should remain between the thresholds in the two-process model, see for example Figure 4. For values between the thresholds, either sleep or wake can occur. Above the upper threshold, only sleep can occur: this could be viewed as a region of sleep, from which it is hard to wake up. Below the lower threshold, only wake can occur, representing times when it is difficult to fall asleep.

Motivated by the strong relationship between the two-process model and the slow dynamics of the PR model, we have re-visited the two-process model. By using that the two-process model can be represented as a one-dimensional map with discontinuities we are able to interpret the transitions from monophasic to polyphasic sleep as grazing bifurcations. This provides the dynamical underpinning for the observation that the PR model gives a systematic framework which encompasses many different mammalian species and confirms the hypothesis of [10] that such a framework could be present in the two-process model. Furthermore, it suggests that ‘typical’ transitions with varying clearance parameter, at least for the larger mammalian species with relatively large clearance parameters, will involve gaining or losing one sleep episode a day. We note that the sequence of transitions for increasing χ is consistent with observations of changes in the daily sleep patterns of early childhood.

Varying the homeostatic time constant as shown in Figure 6(a) suggests that for large mammals (large χ) sleep regulation is dominated by the circadian rhythm. In contrast, as shown in Figure 6(d), small mammals are more strongly driven by their metabolism and it is the homeostatic component that dominates. However, we note that the equivalence of the two models raises some interesting questions on accepted parameter values: in both models the homeostatic process is modelled in a similar way, with exponential decay during sleep and an exponential approach to an upper asymptote during wake. In the context of the two process model, accepted physiological markers for the homeostatic process are slow waves in the sleep EEG and theta activity in the EEG during wake respectively, both of which are readily measured. The time constants χ_s and χ_w differ during wake and sleep and are measured to be $\chi_s \approx 4$ hrs and $\chi_w \approx 18$ hrs in humans [11]. An important physiological question is the necessity for two different time constants for the homeostatic

process, one for wake and one for sleep. Animal [41] and human experiments [42] strongly suggest that the time constant during wakefulness varies with genetic background (animals) and during development (humans) whereas the time constant during sleep appears more invariant within species. In the context of the PR model, the homeostatic process represents the concentration of somnogenic factors such as adenosine, which are not easily accessible. During wake, adenosine is produced more quickly in the brain than it is cleared, decreasing the inhibition to the VLPO. A single value $\chi = \chi_s = \chi_w = 45$ hrs is taken in order to replicate typical sleep patterns for adult humans. Given that in both models, the homeostatic process plays a key role in determining patterns of sleep and wake, it would be interesting to extend the modelling of the homeostatic process in the PR model to allow χ_s and χ_w to differ and determine whether a different parameterization of the PR model would lead to time constants in-line with measured values for the two process model.

The grazing bifurcations have been shown to occur as the clearance parameter χ and as the mean drive to the VLPO or equivalently, both the upper and lower thresholds, are simultaneously varied. However, it is clear that the tangencies between the sleep-wake trajectories and the thresholds that give rise to these bifurcations could also occur if the distance between the thresholds (see [29, 30]) or the upper and lower asymptotes of the homeostatic process are varied. A systematic study will be carried out elsewhere.

The two-process model has been compared with sleep deprivation experiments by assuming that the upper threshold is no longer present and that the sleep pressure continues to increase, with sleepiness linearly related to the difference between the homeostat and the circadian process. Here, we have demonstrated that the notion of ‘wake effort’ introduced in [25] is a similar measure and is equivalent to imagining, not that the upper threshold has vanished, but that increasing the stimulation to the MA results in increasing the upper threshold in line with the increase in H .

Similarly, one could also imagine a ‘sleep effort’ that would be required to keep the model asleep when it would naturally wake. This could be achieved by reducing the lower threshold in the two-process model or, equivalently, decreasing the stimulation to the MA, D_m . As can be seen from Figure 9(b), the PR model parameters suggest that, while it is possible to extend the wake state significantly by increasing D_m , the capacity to extend the sleep state is more restricted. This observation is sensitive to the precise parameters and definition of the firing function. The asymmetry between sleep and wake is equivalent to the fact that in [25], the authors noted that the ‘sleep ghost’ is less prominent than the ‘wake ghost’.

The equivalence between the PR model on the slow timescale and the two-process model is exact when the firing function is a hard switch, but when

the firing function is sigmoidal is more subtle. This is because, in the PR model, the upper/lower asymptotes of the homeostatic process are modelled as a function of Q_m the firing rate of the MA. With a hard switch, Q_m takes only two values, Q_S or zero (similar to the two-process model), but with a sigmoid it varies continuously. Except in the neighbourhood of bifurcations, for monophasic sleep we have shown that one can fix the maximal value of Q_m and the switching voltage θ_S such that the times when the homeostatic pressure reaches its extreme values in the PR and two-process models coincide. The precise values of Q_m and θ_S needed, and therefore the values of the asymptotes in the equivalent two-process model, depend to some extent on the other parameters in the model. In this paper we have taken the approach of fixing the values of the asymptotes as those needed to agree with the PR model for their ‘normal’ values of the parameters at $\chi = 45$. We have not then varied the asymptotes as other parameters are changed which means that the quantitative agreement between the results from the two-process model and the PR model are not exact. Nevertheless, the sequence of transitions and the underlying mechanism through grazing bifurcations carry over between the two models with only minor quantitative differences. In the case of the wake effort, the dependence of the upper asymptote on the firing rate in the PR model means that there is approximately a 10% difference in the wake effort between the two-process and PR models after four days.

However, the fact that implicit in the PR model is a non-constant asymptotic value for the homeostatic process has wider implications. Sleep deprivation experiments tend to show a leveling off of psychomotor vigilance test (PVT) scores over a period of a few days, similar to the levelling off seen in the wake effort shown in Figure 10. In contrast, chronic sleep restriction experiments, where subjects repeatedly are allowed less sleep than they need, tend to show a linear increase in PVT over the timescale of typical experiments. In order to explain this, in [13], Avinash *et al* considered a two-process model but suggested that the upper and lower asymptotes varied with time. This idea was generalised in [14]. Both papers suggest that the time variation occurs through some longer timescale process. We note that within the context of the PR model, during sleep deprivation or chronic sleep restriction the values of the firing function will tend to increase, automatically inducing some time dependence in the values of the asymptotes.

The asymptotes and therefore the wake effort in the PR model are sensitive to the particular choice of the firing function and the functional dependence of the upper asymptote on Q_m . For parameter choices made in [25], Q_m , like D_m , depends approximately linearly on wake effort. However, note that the shape of the relation between D_v and D_m shown in Figure 9 means

that for high D_m there is a ‘corner’ where to stay awake longer means that a very large increase in D_m is needed. This transition suggests that a critical change in behaviour for large wake effort, although it is unclear whether this could give an alternative explanation for the behaviour at extreme sleep restriction to the ‘bifurcation’ suggested by [14]. This corner can be further understood by re-examining the firing function shown in Figure 3. Since only a small part of the sigmoid is used under ‘normal’ conditions for the PR model, increasing D_m will result in an almost linear change to the range of Q_m . However, once D_m is large, it becomes increasingly difficult to increase Q_m by increasing D_m and the corner in Figure 9 corresponds to the flattening off of the relationship between Q_m and D_m . While this is beyond the physiological range of the parameters, this part of the PR model has been less constrained by physiological parameters or behaviour than many other features of the model and a slightly different firing function could lead to a corner at more physiological values. The relationship between the two-process based model in [14], the PR model and the modelling of sleep deprivation versus sleep restriction deserves further attention and will be the subject of a future paper.

In order to better understand sleep/wake regulation it is essential that models that incorporate neurophysiology are developed, analysed and used. However, as models become more complex two problems arise. Firstly they become difficult to analyse systematically, with large numbers of numerical simulations becoming the principle method used to establish the behaviour of the system. Secondly, there is a proliferation of parameters which cannot be easily determined experimentally. One consequence is that it becomes difficult to establish the relative merits of different models. By demonstrating that the two-process model and the PR model are essentially the same for sleep-wake phenomena on the slow time-scale of hours we have not only gained insight on the interpretation of both models but also established the mechanism for transitions between different patterns of sleep and wake in the PR model. This link also suggests some interesting avenues for future extensions of the PR model based on recent insights and research on the two-process and related models.

Acknowledgements

This work was partially supported by the Engineering and Physical Sciences Research Council (grant number EP/I000992/1) and by the Royal Society of Medicine (DJD).

References

- [1] F.P. Cappuccio, L. D’Elia, P. Strazzullo, and M.A. Miller. Sleep duration and all-cause mortality: a systematic review and meta-analysis of prospective studies. *Sleep*, 33:585–592, 2010.
- [2] K. L. Knutson. Sleep duration and cardiometabolic risk: a review of the epidemiologic evidence. *Best. Pract. Res. Clin. Endocrinol. Metab.*, 24:731–743, 2010.
- [3] F.P. Cappuccio, D. Cooper, L. D’Elia, P. Strazzullo, and M.A. Miller. Sleep duration predicts cardiovascular outcomes: a systematic review and meta-analysis of prospective studies. *Eur. Heart J.*, 32:1484–1492, 2011.
- [4] L. S. Nielsen, K.V. Danielsen, and T.I. Sorensen. Short sleep duration as a possible cause of obesity: critical analysis of the epidemiological evidence. *Obes. Rev.*, 12:78–92, 2011.
- [5] E. Kronholm, M. Sallinen, P. Era, T. Suutama, R. Sulkava, and T. Partonen. Psychomotor slowness is associated with self-reported sleep duration among the general population. *Journal of Sleep Research*, 20:288–297, 2011.
- [6] C. S. Möller-Levet, S. N. Archer, G. Bucca, E. E. Laing, A. Slak, R. Kabiljo, J. C. Y. Lo, N. Santhi, M. von Schantz, and D.J. Dijk. Effects of insufficient sleep on circadian rhythmicity and expression amplitude of the human blood transcriptome. *Proceedings of the National Academy of Sciences*, 2013.
- [7] S. Archer, E.E. Laing, C.S. Möller-Levet, D.R van der Veen, G. Bucca, A.S. Lazar, N. Santhi, A. Slak, R. Kabiljo, M. von Schantz, C.P. Smith, and D.-J. Dijk. Mistimed sleep disrupts circadian regulation of the human transcriptome. *Proceedings of the National Academy of Sciences*, 111:E682–91, 2014.
- [8] M.C. Moore-Ede and C.A. Czeisler, editors. *Mathematical models of the circadian sleep-wake cycle*. Raven Press, New York, 1984.
- [9] A. Borbély. A two process model of sleep regulation. *Human Neurobiology*, 1:195–204, 1982.
- [10] S. Daan, D.G.M. Beersma, and A.A. Borbely. Timing of human sleep: recovery process gated by a circadian pacemaker. *Am. J. Phys*, 246:161–178, 1984.

- [11] A. Borbély and P. Achermann. Sleep homeostasis and models of sleep regulation. *Journal of Biological Rhythms*, 14:559–570, 1999.
- [12] M.H. Hagenauer and T.M. Lee. Adolescent sleep patterns in humans and laboratory animals. *Hormones and Behaviour*, 64:270–279, 2013.
- [13] D. Avinash, C.P. Crudele, D.D. Amin, B.M. Robinson, D.F. Dinges, and H.P.A. van Dongen. Parameter estimation for a biomathematical model of psychomotor vigilance performance under laboratory conditions of chronic sleep restriction. *Sleep-Wake research in the Netherlands*, 16:39–42, 2005.
- [14] P. McCauley, L.V. Kalachev, A.D. Smith, G. Belenky, D.F. Dinges, and H.P. Van Dongen. A new mathematical model for the homeostatic effects of sleep loss on neurobehavioral performance. *Journal of Theoretical Biology*, 256:227–39, 2009.
- [15] Y. Tamakawa, A. Karashima, Y. Koyama, N. Katayama, and M. Nakao. A quartet neural system model orchestrating sleep and wakefulness mechanisms. *J. Neurophysiol.* /, 95:2055–69, 2006.
- [16] C.G. Diniz Behn, E. Brown, T. Scammell, and N. Kopell. A mathematical model of network dynamics governing mouse sleep-wake behavior. *Journal of Neurophysiology*, 97:3828–40, 2007.
- [17] A.J.K. Phillips and P.A. Robinson. A quantitative model of sleep-wake dynamics based on the physiology of the brainstem ascending arousal system. *J. of Biol. Rhythms*, 22:167–179, 2007.
- [18] S. Postnova, K. Voigt, and H.A. Braun. A mathematical model of homeostatic regulation of sleep-wake cycles by hypocretin/orexin. *J. Biol. Rhythms*, 24:523535, 2009.
- [19] C.G. Diniz Behn and V. Booth. Simulating microinjection experiments in a novel model of the rat sleep-wake regulatory network. *Journal of Neurophysiology*, 103:1937–1953, 2010.
- [20] M.J. Rempe, J. Best, and D. Terman. A mathematical model of the sleep/wake cycle. *J. Math. Biol.*, 60:615–644, 2010.
- [21] V. Booth and C.G. Diniz Behn. A fast-slow analysis of the dynamics of REM sleep. *SIAM Journal of Applied Dynamical Systems*, 11:212–242, 2012.
- [22] V. Booth and C.G. Diniz Behn. Physiologically-based modeling of sleep-wake regulatory networks. *Mathematical Biosciences*, 250:54–68, 2014.

- [23] B.D. Fulcher, A.J.K. Phillips, and P.A. Robinson. Modeling the impact of impulsive stimuli on sleep-wake dynamics. *Phys. Rev. E*, 78:051920, 2008.
- [24] A.J.K. Phillips, P.A. Robinson, D.J. Kedziora, and R.G. Abeysuriya. Mammalian sleep dynamics: how diverse features arise from a common physiological framework. *PLoS Comp. Biol.*, 6:e1000826, 2010.
- [25] B.D. Fulcher, A.J.K. Phillips, and P.A. Robinson. Quantitative physiologically based modeling of subjective fatigue during sleep deprivation. *J. Theor. Biol.*, 264:407–419, 2010.
- [26] M. Puckeridge, B.D. Fulcher, A.J.K. Phillips, and P.A. Robinson. Incorporation of caffeine into a quantitative model of fatigue and sleep. *J. Theor. Biol.*, 273:44–54, 2011.
- [27] A.J.K. Phillips, P.Y. Chen, and P.A. Robinson. Probing the mechanisms of chronotype using quantitative modeling. *J. Biol. Rhythms*, 25:217–227, 2010.
- [28] A.J.K. Phillips, C.A. Czeisler, and E.B. Klerman. Revisiting spontaneous internal desynchrony using a quantitative model of sleep physiology. *J. Biol. Rhythms*, 26:441–453, 2011.
- [29] M. Nakao, H. Sakai, and M. Yamamoto. An interpretation of the internal desynchronizations based on dynamics of the two-process model. *Methods Inf. Med.*, 36:282–5, 1997.
- [30] M. Nakao and M. Yamamoto. Bifurcation properties of the two process model. *Psychiatry Clin. Neurosci.*, 52:131–3, 1998.
- [31] A.J.K. Phillips and P.A. Robinson. Sleep deprivation in a quantitative physiologically based model of the ascending arousal system. *J. Theor. Biol.*, 255:413–423, 2008.
- [32] R. M. May. Simple mathematical models with very complicated dynamics. *Nature*, 261(5560):459–467, 1976.
- [33] H.E. Nusse and J.A. Yorke. Border collision bifurcations including “period two to period three” for piecewise smooth systems. *Psychiatry Clin. Neurosci.*, 57:39–57, 1992.
- [34] T. LoFaro. Period-adding bifurcation in a one parameter family of interval maps. *Mathematical and Computer Modelling*, 76:27–41, 1996.

- [35] P. Jain and S. Banerjee. Border-collision bifurcations in one-dimensional discontinuous maps. *International Journal of Bifurcation and Chaos*, 13:3341–3351, 2003.
- [36] T. LoFaro and N. Kopell. Timing regulation in a network reduced from voltage-gated equations to a one-dimensional map. *Journal of Mathematical Biology*, 38:479–533, 1999.
- [37] S. Coombes and A. H. Osbaldestin. Period-adding bifurcations and chaos in a periodically stimulated excited beural relaxation oscillator. *Physical Review E*, 24:4057–4066, 2000.
- [38] V. Avrutin, M. Schanz, and S. Banerjee. Multi-parametric bifurcations in a piecewise-linear discontinuous map. *Nonlinearity*, 19:1875–1906, 2006.
- [39] D.-J. Dijk and C.A. Czeisler. Contribution of the circadian pacemaker and the sleep homeostat to sleep propensity, sleep structure, electroencephalographic slow waves, and sleep spindle activity in humans. *J. Neurosci*, 15:3528–3538, 1995.
- [40] P. Achermann and A. Borbély. Mathematical models of sleep regulation. *Front. Biosc.*, 8:683–693, 2003.
- [41] P. Franken, D. Chollet, and M. Tafti. The homeostatic regulation of sleep need is under genetic control. *Journal of Neuroscience*, 21:2610–2621, 2001.
- [42] O.G. Jenni, P. Achermann, and M.A. Carskadon. Homeostatic sleep regulation in adolescents. *Sleep*, 28:1446–1454, 2005.

A Parameter values

Parameter	PR	PR switch
Q_{\max} or Q_S	100s^{-1}	4.85s^{-1}
θ	10mV	1.45mV
σ'	3mV	-
ν_{vm}	2.1mVs	0.208mVs
ν_{mv}	1.8mVs	1.8mVs
ν_{vc}	2.9mV	2.9mV
ν_{vh}	1mVnM^{-1}	1mVnM^{-1}
A_m	1.3mV	1.5mV
A_v	13.05mV	13.05mV
τ_m	10s	10s
τ_v	10s	10s
χ	45hrs	45hrs
$\bar{\mu}$	4.4nMs	4.4nMs

Table 1: Typical parameter values for the PR model and the equivalent parameters for the PR model with a hard switch: these are needed to find appropriate parameter values for the two-process model. Further details on how to find values of ν_{vm} and Q_S are given in the Supplementary Material. All parameters have been defined to be positive, consequently some of the signs in equations (6) are opposite to their original definitions in [17]. The mean component of the circadian drive in the PR model has been incorporated in the definition of A_v , $A_v = \nu_{vc}c_0$, $c_0 = 4.5$.

B PR switch to two-process comparison

The equations for the PR switch model are

$$\begin{aligned}
 \tau_v \dot{V}_v + V_v &= -\nu_{vm} Q_S \mathcal{H}(V_m - \hat{\theta}_S) + D_v(t) \\
 \tau_m \dot{V}_m + V_m &= -\nu_{mv} Q_S \mathcal{H}(V_v - \hat{\theta}_S) + D_m(t) \\
 \chi \dot{H} + H &= \bar{\mu} Q_S \mathcal{H}(V_m - \theta_S),
 \end{aligned} \tag{11}$$

where

$$\begin{aligned}
 D_v &= \nu_{vh} H - \nu_{vc} C(t) - A_v \\
 D_m &= A_m.
 \end{aligned}$$

Since $\tau \ll \chi$ we introduce the small parameter $\epsilon = \tau/\chi$, the fast time $\hat{t} = t/\epsilon$ and the slow time $T = t$, $d/\hat{d}\hat{t} = \epsilon d/dt$ and $d/dT = d/dt$. Then, at $O(1)$ (slow time) equations (11) become

$$\begin{aligned} V_v &= -\nu_{vm}Q_S\mathcal{H}(V_m - \theta_S) + D_v(T) \\ V_m &= -\nu_{mv}Q_S\mathcal{H}(V_v - \theta_S) + D_m(T) \\ \chi\dot{H} + H &= \bar{\mu}Q_S\mathcal{H}(V_m - \theta_S), \end{aligned} \quad (12)$$

where

$$\begin{aligned} D_v &= \nu_{vh}H - \nu_{vc}C(T) - A_v \\ D_m &= A_m. \end{aligned}$$

During wake, these have solution

$$\begin{aligned} V_v &= -\nu_{vm}Q_S + \nu_{vh}H - \nu_{vc}C(T) - A_v, \\ V_m &= A_m, \\ H &= \bar{\mu}Q_S + (H_0 - \bar{\mu}Q_S)e^{(T_0-T)/\chi}. \end{aligned}$$

During sleep, these have solution

$$\begin{aligned} V_v &= \nu_{vh}H - \nu_{vc}C(T) - A_v, \\ V_m &= -\nu_{mv}Q_S + A_m, \\ H &= H_0e^{(T_0-T)/\chi}. \end{aligned}$$

Transitions between wake and sleep when $V_m = \theta_S$, so the switch from wake to sleep occurs when

$$H \equiv H^+ = \frac{\theta_S + A_v + \nu_{vm}Q_S + \nu_{vc}C(T)}{\nu_{vh}},$$

and from sleep to wake when

$$H \equiv H^- = \frac{\theta_S + A_v + \nu_{vc}C(T)}{\nu_{vh}}.$$

By comparison with equations (1)-(4) we see that the two-process model and the dynamics of the PR switch model on the slow manifold are equivalent if

$$\begin{aligned} H_0^+ &= \frac{\theta_S + A_v + \nu_{vm}Q_S}{\nu_{vh}}, & H_0^- &= \frac{\theta_S + A_v}{\nu_{vh}}, \\ a &= \frac{\nu_{vc}}{\nu_{vh}}, & \mu &= \bar{\mu}Q_S, & \chi_s &= \chi_w = \chi. \end{aligned} \quad (13)$$

For the values of the PR parameters listed in Appendix A and used in Figure 4,

$$H_0^+ = 15.5, \quad H_0^- = 14.5, \quad a = 2.9, \quad \mu = 21.4, \quad \chi_s = 45\text{hrs}, \quad \chi_w = 45\text{hrs}.$$

It is also necessary to take $A_m > \theta_S$, otherwise no switching occurs.

C PR to two-process comparison

On the slow manifold, the PR model is

$$\begin{aligned} V_v &= -\nu_{vm}Q_m + D_v(T) \\ V_m &= -\nu_{mv}Q_v + D_m \\ \chi \frac{dH}{dt} + H &= \bar{\mu}Q_m \end{aligned}$$

where $Q_j, j = m, v$ is given by equation (5). For a fixed value of D_v these have one or three solutions, with the transition between one and three solutions happening at saddle-node bifurcations, D_v^\pm that satisfy

$$\begin{aligned} D_v^\pm &= V_v - \nu_{vm}Q_m \\ D_m^\pm &= V_m - \nu_{mv}Q_v \\ \frac{\nu_{vm}\nu_{mv}}{\sigma'^2} &= (Q_v - Q_{\max})(Q_m - Q_{\max}). \end{aligned} \tag{14}$$

The values of D_v^\pm depend on $\nu_{vm}, \nu_{mv}, Q_{\max}, \sigma'$ and θ , and for the values commonly used in the PR model and listed in Table 1 give $D_v^+ = 2.46$ and $D_v^- = 1.45$.

The sleep-wake cycle corresponds to slowly changing D_v , tracing out a path on the slow manifold as shown in Figure 9(a). Transitions from wake to sleep and from sleep to wake occur close to D_v^+ and D_v^- respectively. In order to find parameter values that retain the maximum and minimum values and timings for the homeostatic process for monophasic sleep away from bifurcation points the following algorithm is followed:

- First the identification between the threshold values and the saddle node bifurcations in the PR model is made, leading to

$$H_0^+ = \frac{D_v^+ + A_v}{\nu_{vh}}, \quad H_0^- = \frac{D_v^- + A_v}{\nu_{vh}},$$

then

$$H_0^+ - H_0^- = \frac{D_v^+ - D_v^-}{\nu_{vh}}.$$

- Numerically integrating the PR model during monophasic sleep results in trajectories for the homeostat that increase to a maximum during wake and decrease to a minimum during sleep. The maximum and minimum values occur close to the switches from wake to sleep and sleep to wake respectively. During wake, the BDB model gives

$$H(t) = \mu + (H_{\min} - \mu) e^{(t_{\min} - t_{\max})/\chi_w}.$$

Hence, taking

$$\mu = \frac{H_{\max} - H_{\min} \exp\left(\frac{t_{\min} - t_{\max}}{\chi_w}\right)}{1 - \exp\left(\frac{t_{\min} - t_{\max}}{\chi_w}\right)} = 21.35,$$

results in a trajectory for the BDB model that passes through the required values at the required times.

- One can do a similar matching for the decreasing H phase to find a value for the lower asymptote. For the simulations presented here, the value of zero was taken for the lower asymptote.

By integrating the PR model with the ‘normal’ parameter values listed in Appendix A, it is found that the minimum occurs at $H_{\min} = 12.51$, $t_{\min} = 15.31$ hours and the maximum at $H_{\max} = 15.07$, $t_{\min} = 30.67$ hours.

- Comparing the expression for H_0^- above with that for the PR switch model in (13), gives

$$\theta_S = D_v^-.$$

- The relation for Q_S in (13) gives

$$Q_S = \frac{\mu}{\bar{\mu}}.$$

- Considering $H_0^+ - H_0^-$ as given above with H_0^+ and H_0^- as in (13), leads to

$$\nu_{vm} Q_S = D_v^+ - D_v^-.$$

Hence for the typical values of the PR parameters listed in Table 1 and used in Figure 4,

$$\theta_S = 1.45, \quad Q_S = 4.85 \quad \nu_{vm} = 0.208.$$

It is also necessary to take $A_m > \theta_S$ in the PR switch model, otherwise no switching occurs.

Mathematical Models for Sleep-Wake Dynamics: Comparison of the Two-Process Model and a Mutual Inhibition Neuronal Model

Supplementary material

A.C. Skeldon*, D.-J. Dijk†, G. Derks*

* Department of Mathematics, University of Surrey, Guildford, Surrey, GU2 7XH,

† Faculty of Health and Medical Sciences, University of Surrey, Guildford, Surrey, GU2 7XH.

July 15, 2014

The two-process model as a one-dimensional map

As discussed in Section 4, the two-process model can be represented as a one dimensional map with discontinuities. The map is given by

$$T_0^{n+1} = G(T_0^n) \quad (1)$$

where $G(T_0^n)$ is defined as follows. For $t \in (T_0^n, T_w^n]$

$$\begin{aligned} H(t) &= (H_0^+ + aC(T_0^n)) e^{(T_0^n - t)/\chi_s}, \\ T_w^n &= \min(t) \quad \text{s.t.} \quad H(t) = H_0^- + aC(t). \end{aligned}$$

For $t \in (T_w^n, T_0^{n+1}]$

$$\begin{aligned} H(t) &= \mu + ((H_0^- + aC(T_w^n)) - \mu) e^{(T_w^n - t)/\chi_w}, \\ T_0^{n+1} &= \min(t) \quad \text{s.t.} \quad H(t) = H_0^+ + aC(t), \end{aligned}$$

where $C(t) = \cos(\omega(t - \alpha))$; H_0^\pm are the mean values for the upper/lower thresholds; μ is the upper asymptote; χ_s and χ_w are the time constants for the homeostatic process during sleep and wake; a, ω and α are the amplitude, frequency, phase shift, of the circadian process $C(t)$.

In [27] a detailed analysis of piecewise-linear discontinuous maps is presented. It is argued that these represent the normal forms for many systems in the neighbourhood of the discontinuity and that three different bifurcation scenarios are observed in such systems. Of the three scenarios, the particular case that is relevant for the two-process model parameters used to

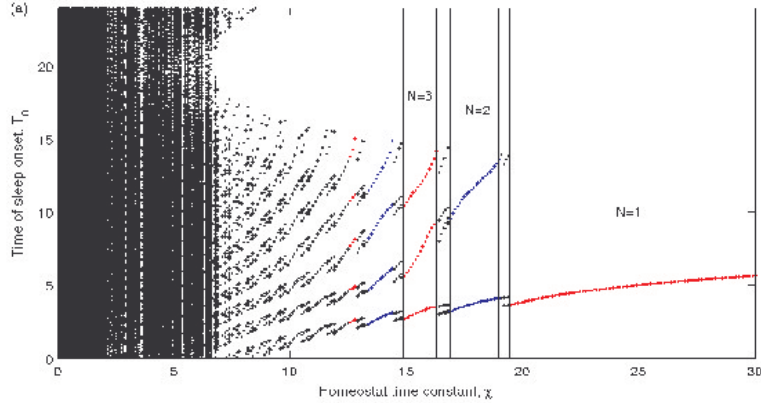


Figure S1: Bifurcation diagram showing the times of sleep onset against the clearance parameter χ in the two-process model. Regions of parameter space where one, two and three daily sleep episodes (N) are delineated but not for higher values for clarity.

match the PR model in this paper is the scenario labelled as period adding bifurcations. It is not yet clear whether the two other scenarios, which [27] label as period increment with coexistence of attractors and pure period increment scenarios, can also occur.

The sequence of bifurcations shown in Figure 6(e) is typical of period adding bifurcations. A more conventional way to present the bifurcation diagram is shown in Figure S1 where the values of T_0^n are plotted against the bifurcation parameter. The term ‘period-adding’ refers to the fact that the period of the iterated map changes as a function of the parameter. So, for example, when the number of daily sleep episodes changes from one to two, the map repeats itself after two iterations.

In the main body of the text it is highlighted that between parameter values where solutions with N daily sleep episodes and solutions with $N + 1$ daily sleep episodes there are solutions which alternate between N and $N + 1$ sleep episodes, as shown in Figure 7. The same sequence occurs in the PR model, as illustrated in Figure S2.

Yet another way of presenting the bifurcation diagram for the iterated map is to plot the length of the daily sleep episodes. This is shown in Figure S3. On this diagram is also plotted the mean daily total sleep. This shows that for the two-process model, as for the PR model, the mean total daily sleep is approximately independent of the homeostatic time constant.

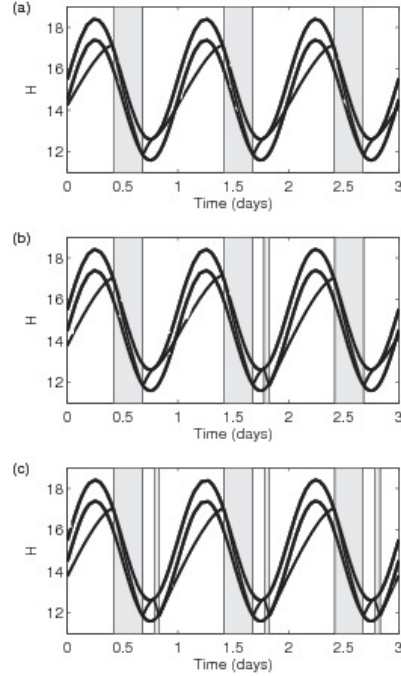


Figure S2: PR model transitions from monophasic to biphasic sleep patterns as χ is reduced. (a) $\chi = 16$ hrs, (b) $\chi = 15.9$ hrs, (c) $\chi = 15.8$ hrs.

The upper asymptote

In Appendix C, it is shown how to fit the parameter μ of the two-process model such that the homeostatic switching happens with the same timing as in the PR model. This fitting is dependent on the sleep-wake cycle and if χ varies, this sleep wake cycle will slightly vary and lead to different timings of the homeostat. In its turn, this would lead to a correction for the parameter μ . In Figure S4 the dependence of the parameter μ is depicted for monophasic sleep.

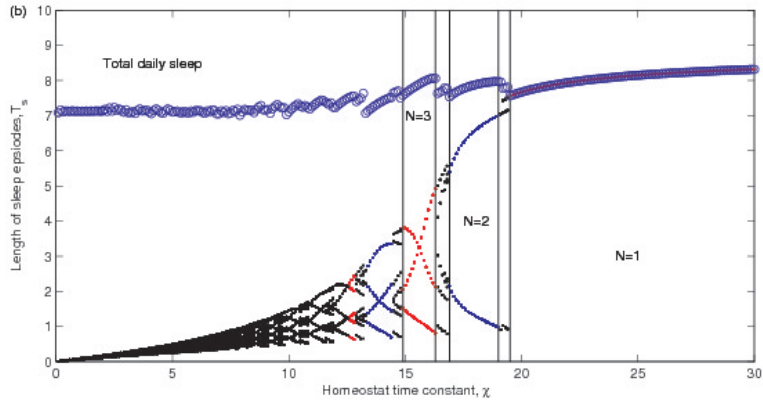


Figure S3: Bifurcation diagram showing length of sleep episode in the two-process model as a function of the parameter χ . So, for example, at $\chi = 22$ hrs there is one single daily sleep episode of length approximately 8 hrs and for $\chi = 18$ hrs there are two daily sleep episodes of approximately 6.6 and 1.5 hrs respectively.

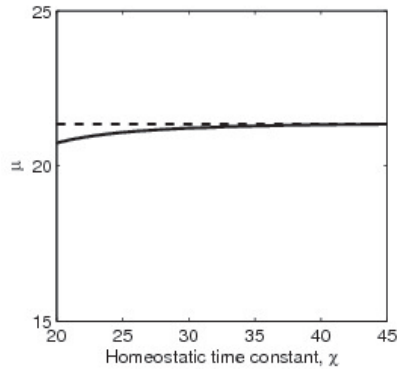


Figure S4: Values of the upper asymptote μ in the two-process model that are needed to fit the PR model for monophasic sleep.